

Low Temperature Green Synthesis of Sulfur-Nitrogen Co-Doped Graphene as Efficient Metal-Free Catalysts for Oxygen Reduction Reaction

Yuan Zhao¹, Chuanxiang Zhang², Tong Liu¹, Rong Fan¹, Yao Sun¹, Haijun Tao¹, Jianjun Xue^{*}

¹ College of Material Science and Science Technology, Nanjing University of Aeronautics and Astronautics, Nanjing 211106, PR China

² College of Materials Engineering, Nanjing Institute of Technology, Nanjing 211167, PR China

*E-mail: jjxue@nuaa.edu.cn

Received: 12 January 2017 / Accepted: 23 February 2017 / Published: 12 March 2017

Development of inexpensive and scalable cathode catalysts that can efficiently catalyze the oxygen reduction reaction (ORR) is of significance in practical application of fuel cells. Heteroatom doped carbons have been recognized as the promising candidate. Herein sulphur-nitrogen co-doped reduced graphene oxide (S-N-rGO) was prepared through low-temperature refluxing with sodium sulfide, ammonia and graphene oxide as the precursors. The catalytic performance of the fabricated S-N-rGO towards the ORR was assessed by electrochemical test. The effect of reaction temperature on catalytic activity was also studied. The S-N-rGO gained under the reaction temperature of 150 °C (S-N-rGO-150 °C) demonstrates higher electrocatalytic activity and mainly four electron ORR process in alkaline condition. In addition, it also shows improved durability and better resistance toward methanol. The excellent performance for the ORR on S-N-rGO is attributed to the synergistic effect originating from the doped S and N in the graphene sheets.

Keywords: co-doped; graphene; oxygen reduction; electrocatalysis; durability

1. INTRODUCTION

With the development of social economic, more and more clean energy is needed to be explored. Owing to the unique advantages of the high power density, excellent energy conversion performance, and low emission of pollutants, Direct Methanol Fuel Cell (DMFC) has been widely concerned by researchers [1-4]. As one of the most important procedure in DMFC, the oxygen reduction reaction (ORR) is proposed to follow two major mechanisms: (1) an efficient four-electron process which involves the formation of H₂O; (2) a two-electron process that produces H₂O₂ as an

intermediate. Generally, the kinetics of ORR is sluggish in nature, so catalysts must be used to boost the efficiency [5-7]. Currently, the most frequently adopted and efficient electrocatalysts are platinum-based catalysts, which was associated with four-electron transfer [8]. However the high cost, limited supply, poor durability as well as less stability of the cathode catalysts have become the biggest obstacle to large-scale commercial application of DMFC [9-11]. Thus, it is urgent to identify non-precious or even metal-free catalysts to reduce or replace the platinum-based catalysts in fuel-cell technologies.

Recently, carbon materials doped with non-metal elements such as nitrogen, sulfur, phosphorus, boron or selenium atoms have been identified as the most popular choice, as a result of its excellent electrocatalytic performance and relatively low costs [4]. Mono-heteroatom doped carbons, especially nitrogen doped graphene and carbon nanotubes have been investigated to show comparable or better oxygen-reduction activity and durability than Pt/C catalyst, the superiority result from enlarged surface areas and enriched high nitrogen doping content [12-14]. Apart from N doped carbons, sulfur (electronegativity of sulfur : 2.58) has a close electronegativity to carbon (electronegativity of carbon : 2.55) [15,16], sulfur-doped graphene by directly annealing graphene oxide and benzyldisulfide in argon also exhibited excellent catalytic activity, long-term stability, and high methanol tolerance [17].

Based on the investigation, carbon materials doped with dual or multi heteroatoms have also been developed. Because of two different heteroatoms co-doped carbons can conjugate into carbon system to change the electronic structure or create new-electron-neutral sites, changing the distribution of electron density and improving the electron spin density, it has been confirmed to be effective for activity enhancement in ORR [18-23]. For instance, B/N co-doped graphene has been demonstrated to show excellent ORR performance in alkaline solution [22]. Likewise, P/N [24, 25], S/N [26, 27], and S/P/N [21, 28] co-doped carbon materials have also been synthesized and studied. On the other hand, the synthesis methods of heteroatom doped graphene involve chemical vapor deposition (CVD) [13, 29, 30]; thermal annealing with heteroatom-containing precursors or gas (NH_3 , H_2S , CS_2) [20, 26, 31, 32]; hydrothermal or solvothermal heteroatom-containing precursors together with carbon materials [33-36]. These methods usually suffer from complicated manipulation, high production cost, low production, which encumbers their large scale production and application in fuel cells. It is still of paramount importance to develop a facile approach towards the synthesis of doped graphene materials.

In this work, sulphur-nitrogen co-doped graphene was successfully synthesized using a green, low temperature and scalable method. To be specific, sodium sulfide and ammonia were chosen as the precursors which are readily available materials with high sulfur and nitrogen content. Under the reduction of sodium sulfide, the hydroxyl and carboxyl of graphene oxide was recovered and many defects appeared. Meanwhile, S and N in the sodium sulfide and ammonia doped into reduced graphene oxide layers, thus the S-N co-doped reduced graphene oxide formed. Upon measuring the properties of as-prepared catalysts, it was found that S-N-rGO exhibited excellent electrocatalytic activity and better potential prospect than commercial Pt/C catalysts. Which indicated S-N-rGO will be a promising candidate as low-cost, metal-free electrochemical catalysts for ORR in alkaline media. Moreover the catalysis is common, cheap, and nontoxic to environment, so this S-N-rGO is suitable for large-scale preparation for industrial applications.

2. MATERIALS AND METHODS

2.1. Materials

Sulfuric acid (H_2SO_4), phosphoric acid (H_3PO_4), potassium permanganate (KMnO_4), hydrogen peroxide (H_2O_2) and ammonia ($\text{NH}_3 \cdot \text{H}_2\text{O}$) were obtained from Sinopharm Chemical Reagent Co., Ltd. (Shanghai, China). sodium sulphide (Na_2S) were purchased from Aladdin Industrial Corporation (China). Unless otherwise stated, all the reagents were of analytical grade and were used as received without further purification, all the solutions used in electrochemical experiments were prepared with ultrapure water ($18.3 \text{ M}\Omega \text{ cm}^{-1}$)

2.2. Preparation of nitrogen/sulfur co-doped graphene

Graphite oxide (GO) was synthesized from natural graphite flakes by a modified Hummers method [37]. In brief, 1 g natural graphite was added into a flask containing 45 mL of concentrated sulfuric acid and 5 mL of concentrated phosphoric acid, the flask was then placed in an ice bath. Next, 7 g KMnO_4 was slowly added under stirring while keeping the temperature below 20°C . The flask was then heated to 50°C and maintained for 12 h. After cooling to room temperature, 100 mL of deionized water and 2 mL of 35% H_2O_2 were successively dropped into mixture under ice bath condition. As a result, residual KMnO_4 and MnO_2 were reduced to Mn^{2+} , the color of the products changed from dark brown to bright yellow, which indicated the formation of graphite oxide from graphite. Subsequently, the obtained bright yellow solution was centrifuged to collect the solid product at the bottom. To remove impurity ions in the precipitate, a washing step was taken with 37% HCl and lots of deionized water, until the pH value of the suspension was about [7]. The mixtures were finally freezing-dried and stored in a drying cabinet. Characterizations of graphite oxide were listed in the supporting.

S-N-rGO was prepared by low-temperature refluxing technique. The preparation of the specific process was as follows: 0.5 g graphite oxide and 3 mL ammonia were ultrasonically dispersed in 250 mL water for 30 min, then 2 g Na_2S was added. The solution was filled in a mouth flask and placed into oil bath. Then oil was heated to 150°C for 16 h with the cold water flow after which was allowed to cool down to room temperature. Balloon is used to buffer the pressure in system. The resulting production was separated through filtration with a microporous membrane (pore size $0.45 \mu\text{m}$) and washed with deionized water, afterwards it was dried in vacuum freeze drying overnight. Schematic illustration of the synthesis of S-N co-doped graphene was shown in Fig.1. The resulting materials were denoted as S-N-rGO- 50°C , S-N-rGO- 100°C , S-N-rGO- 150°C , S-N-rGO- 180°C for different reaction temperature. The synthetic procedure of S-rGO and N-rGO are the same with that for preparing S-N-rGO, the only difference is that no ammonia or Na_2S was added during the synthesis.

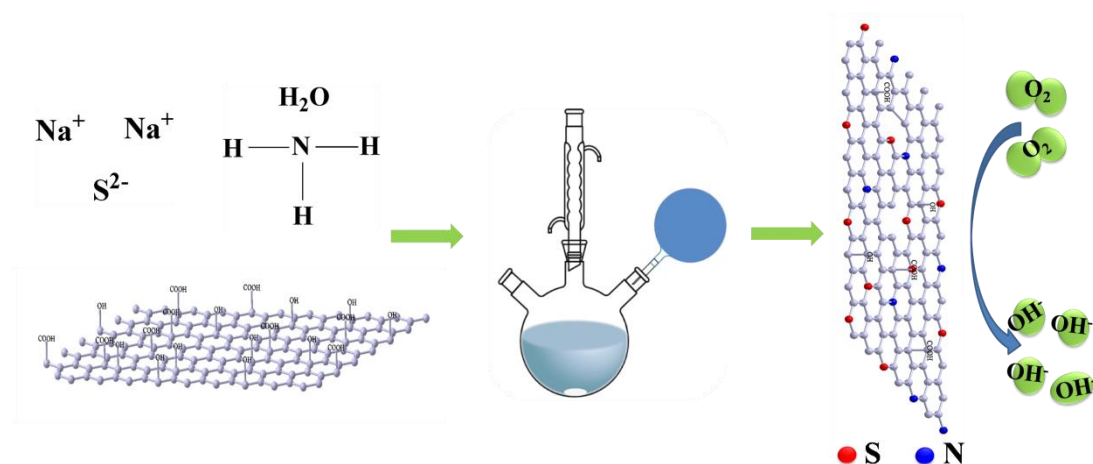


Figure 1. Schematic illustration of the synthesis of S-N co-doped reduced graphene oxide.

2.3 Characterization and measurements

Glass carbon (GC) electrode (5 mm diameter) was polished with a 0.05 μm alumina slurry and subsequently rinsed with ultrapure water and ethanol. The electrodes were then sonicated in ultrapure water, rinsed thoroughly with ultrapure water and ethanol and dried under room temperature. For working electrode preparation, 5 mg S-N-rGO were dispersed in 1 mL solvent mixture of Nafion (5%) and ethanol (V:V ratio=1: 9) for 0.5 h under sonication. And then 25 μL portion of the resulting suspension was dropped onto the GC surface and dried at room temperature. For comparison, a commercially available catalyst of 20% Pt/C was prepared in the same way.

The surface morphologies of composites were investigated by transmission electron microscopy (TEM) (TEM, G2 T20, Tecnai) coupled with energy-dispersive X-ray spectrometer at an accelerating voltage of 200 kV. To prepare the specimen, the as-prepared catalysts were added into 2 mL of ethanol and sonicated for 1 min. The resulting suspension was drop casted onto a piece of a TEM grid. The elements binding environment of the samples were studied with X-ray photoelectron spectroscopy spectrometer (XPS, K-Alpha, Thermo). Calibration of binding energy was carried out by setting binding energy of C1s peak to 284.4 eV. The crystal structure of as-synthesized S-N-rGOs sample was identified by X-ray diffraction (XRD, Ultima IV, Rigaku, Cu Ka, $\lambda=1.54\text{\AA}$). The samples were step-scanned in steps of 0.02° in the range of $10\text{-}90^\circ$ using a counter time of 24 s per step. And Raman spectroscopy (inVia , Renishaw) using the 532 nm laser line of an air cooled Ar-ion laser.

The electrochemical measurements to evaluate ORR activity, including cyclic voltammetry (CV), rotating disk electrode (RDE) and chronoamperometry, were performed on a CHI 660D electrochemical workstation with a three-electrode system. A rotating glass carbon disk after loading the electrocatalyst was used as the working electrode, an saturated calomel electrode as the reference electrode, and a Pt plate as the counter electrode. The cyclic voltammetric experiments were conducted in O_2 -saturated 0.1 M KOH solution for the oxygen reduction reaction with the scan rate of 20 mV/s from -0.8V to +0V at room temperature. Linear sweep voltammetry measurements were performed using RDE at different rotating from 400 to 2025 rpm at a scan rate of 5 mV/s at room temperature after purging O_2 for at least 30min. Long-term stability of catalysts was measured at a constant voltage

of -0.4V in O₂ bubbled 0.1 M KOH electrolytes. The Koutecky–Levich equations shown below were employed to analyze the transferred electron number (*n*) [38]:

$$\frac{1}{J} = \frac{1}{J_L} + \frac{1}{J_K} = \frac{1}{B\omega^{1/2}} + \frac{1}{J_K} \quad (1)$$

$$B = 0.2nFC_0(D_0)^{2/3}\nu^{-1/6} \quad (2)$$

Where *J* is the overall current density, *J_L* is the diffusion-limiting current density, *J_K* is the kinetic current density, ω is the angular velocity of the disk ($\omega = 2\pi N$, *N* is the linear rotation speed), *F* is the Faraday constant (*F* = 96485C mol⁻¹), *C₀* is the bulk concentration of O₂ (*C₀* = 1.2 × 10⁻⁶ mol cm⁻³), *D₀* is the diffusion coefficient of O₂ (1.9 × 10⁻⁵ cm² s⁻¹), ν is the kinematics viscosity of the electrolyte ($\nu = 0.01$ cm² s⁻¹) and *n* is the overall number of electrons transferred in oxygen reduction. According to equation (1) and (2), the number of electrons transferred (*n*) can be obtained from the slope of the Koutecky–Levich plots, respectively.

3. RESULTS AND DISCUSSION

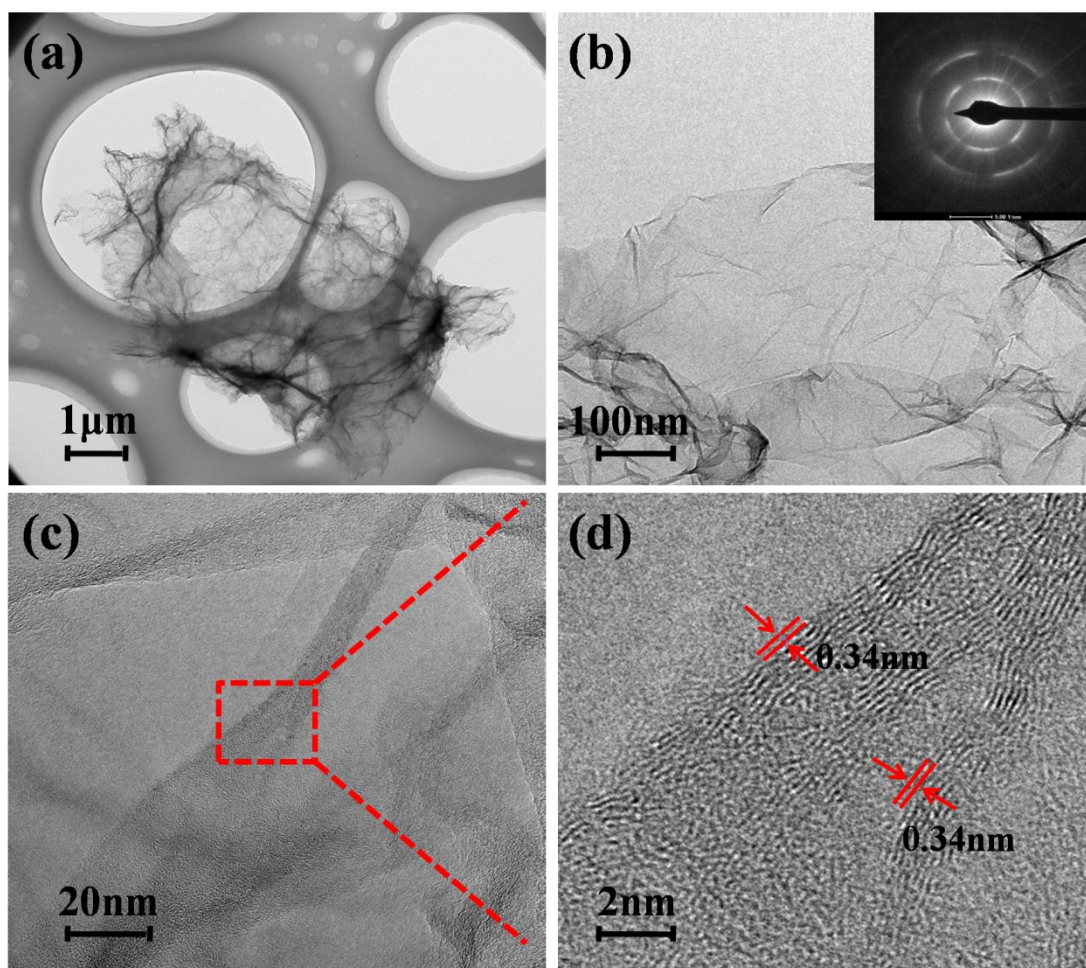


Figure 2. (a) TEM image of S-N-rGO and (b) TEM image and the corresponding selected-area electron diffraction pattern; (c) HRTEM image of S-N-rGO; (d) HRTEM of crumple zone in(c).

The as-prepared S-N-rGO-150 °C was characterized by means of transmission electron microscopy (TEM) and high-resolution transmission electron microscopy (HRTEM). As shown in Fig. 2(a) graphene sheets seem as a silk handkerchief in the case of low magnification, a crumpled, cross-linked but still transparent thin film are obtained in Fig. 2(b). The partially crinkled nature originate from the defective structures formed during the fabrication of GO and the heteroatom doping process. The selected-area electron diffraction (SAED) pattern (Fig. 2b) shows that the width of diffraction point is caused by a large number of wrinkles. As shown in Figure 2(c), most of the S-N-rGO is crumpled and contains entangled wrinkles. These layers show a layer distance of about 0.34 nm but with poor crystallite, which is corresponding with the theoretical thickness of a single-layer graphene (0.34 nm).

The elemental composition and chemical status of the S-N-rGO were investigated by XPS. The survey spectrum shown in Fig. 3(a) unveils the presence of C, O, N, S with the content of 84.03%, 11.49%, 3.65% and 0.84%, respectively. And the high-resolution C1s, N1s, and S2p spectra were collected to find out whether the N and S atoms have been successfully doped into the lattice of reduced oxide graphene. As shown in Fig3 (b), the high resolution spectrum of C1s can be deconvoluted into three peaks, corresponding to C-C (284.8 eV), C-S & C-O (286.0 eV) and C-N & C=O (287.1 eV) bonding [27,35], which is just more proof that the N and S are doped into graphene framework rather than physically adsorbed on the graphene sheets. The high-resolution N1s spectrum (Fig. 3(c)) shows that the presence of two types of N atoms, according with pyrrolic N (400.2 eV) and pyridinnic N (398.2 eV). It is interesting to note that 69% of the total N in S-N-rGO is of pyridinic in nature and is considered to be the most active site for catalytic reduction of oxygen [39]. The S2p spectrum of S-N-rGO is displayed in fig. 3(d) The three peaks in Fig.3c are attributed to S2p 3/2 (163.8 eV) and S2p 1/2 (165 eV) and SO_x groups (168.8 eV) [40,41]. The -C-S_n-C- and -C=S- bondings are the characteristic of thiophene-S owing to their spinorbit coupling, which has been designed to functionalize various species into the carbon frameworks toward high performance materials. And the SO_x groups are not active for oxygen reduction reaction [17,42]. In this work we used simple and effective method to successfully introduce S and N atoms into the carbon framework via covalent bonds. In fact, Dai's report clearly indicates that carbon materials can react with NH₃ to form C-N bonds [43]. Hence, it is bold trial to tentatively speculate that C-S bond in the samples formed through a similar mechanism.

The X-ray diffraction (XRD) patterns of the as-synthesized S-N-rGO is shown in Fig 4, the samples exhibit two obvious diffraction peaks at $2\theta=24^\circ$ and 44° , corresponding to (002) and (100) reflections of the carbon phase, respectively. Moreover, the (002) and (100) diffraction peaks of S/N-rGO become broader as compared to GO, indicating that additional N and S doping induce more defect sites and disorders in carbon structure [28]. The structural defects in the samples were further studied by Raman spectroscopy. The as-synthesized S-N-rGO and GO samples exhibit two conspicuous peaks at about 1350 cm^{-1} and 1580 cm^{-1} , corresponding to D-band and G-band, respectively. The values of I_D/I_G for samples are also given in Fig 5, The value of I_D/I_G is 0.9006 for GO, 0.9726 for S-N-rGO-50 °C, 1.018 for S-N-rGO-100 °C, 1.045 for S-N-rGO-150 °C, and 1.019 for S-N-rGO-180 °C. Respectively, the highest value of S-N-rGO-150 °C demonstrates that the disorder and defects exist in the sample [44]. The results are in good agreement with those of XRD patterns.

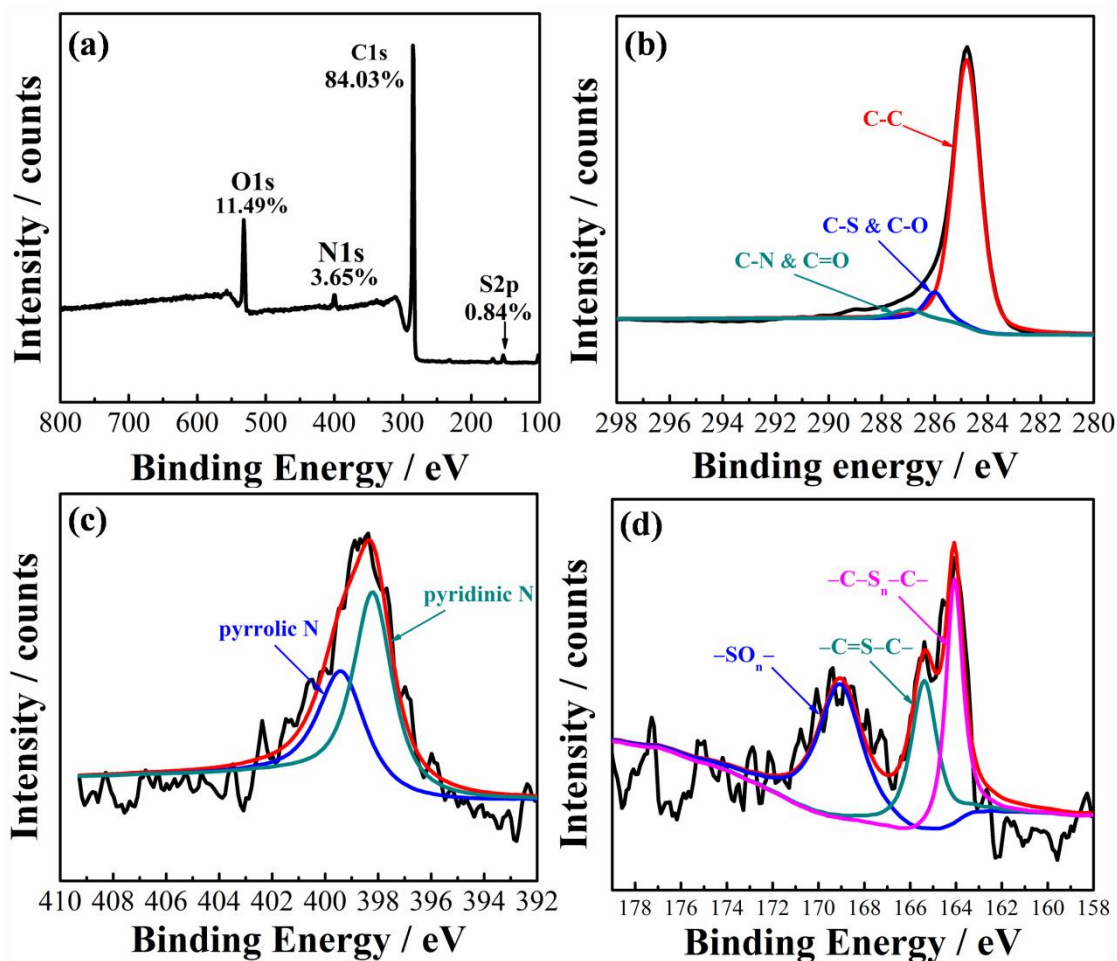


Figure 3. (a) The survey spectra of XPS on S-N-rGO; high resolution of (b) C1s XPS peak; (c) N1s XPS peak;(d) S2p XPS peak.

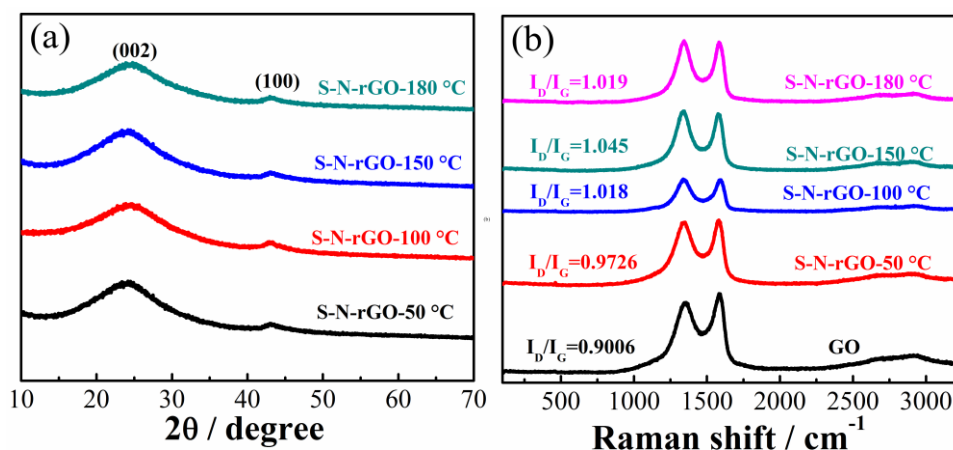


Figure 4. XRD pattern and Raman spectra of S-N-rGO prepared at different temperatures.

To evaluate the influence of dual heteroatom doping for oxygen interaction with doped active sites, the electrocatalytic properties of S-N-rGO were explored. The ORR catalytic activity was assessed by cyclic voltammetry (CV) and linear sweep voltammetry (LSV) in 0.1M KOH solution. A

comparison of N/S-rGO with S-rGO and N-rGO was conducted via linear sweep voltammograms at 1600rpm. It can be seen that the LSV performance of S-N-rGO is better than that of S-rGO and N-rGO with respect to both maximum current density and onset potential. The result shows that the dual heteroatom doping is more advantageous to the reduction of oxygen(Fig. 5). Afteward the electrocatalytic activities of S-N-rGO were further investigated. The CV at S-N-rGO modified glassy carbon (GC) electrode at a scan rate of 20 mV s^{-1} in N_2 and O_2 saturated 0.1M KOH solution were recorded, respectively. As seen in Fig. 6 (a), In N_2 environment, the CV curve was featureless. In O_2 saturated electrolyte, the sample exhibited the evident ORR activity with a well-defined E peak at $\sim -0.26\text{V}$ (vs.SCE) which can be noted as an oxygen reduction peak. This observation confirms the creation of electron dense active sites on the S-N-rGO surface and the suitability of the as-prepared flexible architecture as metal free electrocatalyst for oxygen reduction reaction. Fig. 6 (b) shows LSVs of different samples recorded at an electrode rotation speed of 1600 rpm. A close inspection of LSV profiles shows similar onset (-0.17V) and half-wave (-0.28V) potentials for S-N-rGO-100 $^\circ\text{C}$, S-N-rGO-150 $^\circ\text{C}$, and S-N-rGO-180 $^\circ\text{C}$, and much more positive than that of S-N-rGO-50 $^\circ\text{C}$. That result suggests S-N-rGO-100 $^\circ\text{C}$, S-N-rGO-150 $^\circ\text{C}$, and S-N-rGO-180 $^\circ\text{C}$ contain similar intrinsic active sites for ORR. The electrocatalytic properties of S-N-rGO catalyst compared to other nitrogen sulphur dual or single doped graphene or other carbon materials previously reported in literatures are shown in Table 1. Based on the results reported, N-S-rGO exhibit comparable or better ORR activity than other catalysts prepared previously. For further perception of the ORR kinetic kinetics, the kinetic current density (J_k) and electron transfer number (n) were analyzed based on RDE tests at various rotating speeds from 400 to 2025 rpm and the K-L equations. It is observed that the current density of ORR increases with the acceleration of rotating speed (Fig. 6 (c)), which is due to the improved diffusion of dissolved oxygen to the surface of modified glass carbon electrode[48]. Generally, the number of exchanged electrons during ORR is calculated through the Koutecky-Levich equation. The Koutecky-Levich (K-L) plot of J^{-1} vs $\omega^{-1/2}$ at a potential of -0.3V on the S-N-rGO electrode (Fig. 6 (d)) exhibits good linearity with the R^2 value of 0.998 (Tal. S2). The number of electron transfers for S-N-rGO-150 $^\circ\text{C}$ is calculated to be 3.86, which indicates a four electron-transfer reaction. The above results further confirm that S-N-rGO is a promising metal-free catalysts with high electrocatalytic activity for ORR.

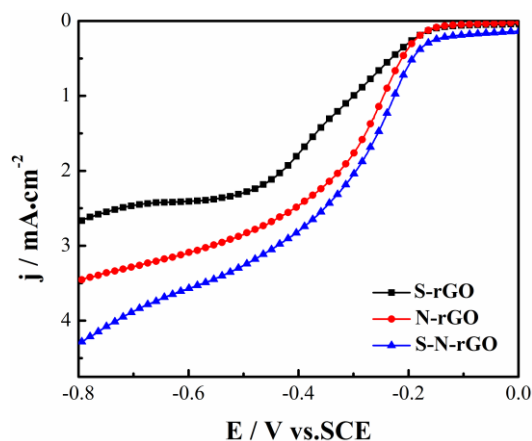


Figure 5 Comparison of LSV curves between S-N-rGO, S-rGO, and N-rGO electrode at 1600 rpm rotation in O_2 -saturated 0.1 M KOH at a scan rate of 5 mV s^{-1}

Table 1. Electrochemical parameters and reaction temperature of S-N-rGO compared to other catalyst for ORR

Catalyst	Reaction Temperature	Eonset (V)	Ehalf-wave (V)	Electrolyte solution	Reference electrode	Reference
N-S-Gas900	900°C	-0.12	-0.24	0.1M KOH	Hg/Hg ₂ Cl ₂	[33]
N-S-Gas800	800°C	-0.21	-0.32	0.1M KOH	Hg/Hg ₂ Cl ₂	[33]
N-S-Gas600	600°C	-0.22	-0.29	0.1M KOH	Hg/Hg ₂ Cl ₂	[33]
NSG700	700°C	-0.15	-0.25	0.1M KOH	Hg/Hg ₂ Cl ₂	[45]
N/S-graphene	800°C	0.002	Not mentioned	1M KOH	Hg/HgO	[26]
Reduced GO	800°C	-0.196	Not mentioned	1M KOH	Hg/HgO	[26]
N-doped graphene	800°C	-0.179	Not mentioned	1M KOH	Hg/HgO	[26]
CA-TCA-900	900°C	-0.18	-0.24	0.1M KOH	Ag/Cl	[46]
rGO/CQDs-HP	180°C	-0.17	Not mentioned	0.1M KOH	Ag/Cl	[47]
CFO/NS-rGO	150°C	-0.13	-0.28	0.1M KOH	Ag/Cl	[34]
NS-rGO	180°C	-0.17	Not mentioned	0.1M KOH	Ag/Cl	[34]
S-graphene	150°C	-0.166	-0.321	0.1M KOH	Hg/Hg ₂ Cl ₂	This work
N-graphene	150°C	-0.172	-0.288	0.1M KOH	Hg/Hg ₂ Cl ₂	This work
S-N-rGO	150°C	-0.159	-0.274	0.1M KOH	Hg/Hg ₂ Cl ₂	This work
20% Pt/C	Commercial product	0.003	-0.125	0.1M KOH	Hg/Hg ₂ Cl ₂	This work

The durability of S-N-rGO toward ORR was evaluated through chronoamperometric measurements at -0.3V. As shown in Fig. 7 (a), the 20000s test only caused 4.3% activity loss on S-N-rGO catalyst. The result is closely to most of reported commercial Pt/C in alkaline solution [14,49]. Concerning the practical application of S-N-rGO in fuel cells, we further test methanol tolerate ability of S-N-rGO and Pt/C catalysts by adding 3M methanol after the chronoamperometric test has run for 60 s. After adding methanol to the electrolyte, the current density of Pt/C catalyst shows a sharp loss of 42% in activity, in contrast, no noticeable change is observed on S-N-rGO (Fig. 7 (b)). The result clearly indicates that the excellent tolerance to methanol for ORR compare with that of conventional Pt/C.

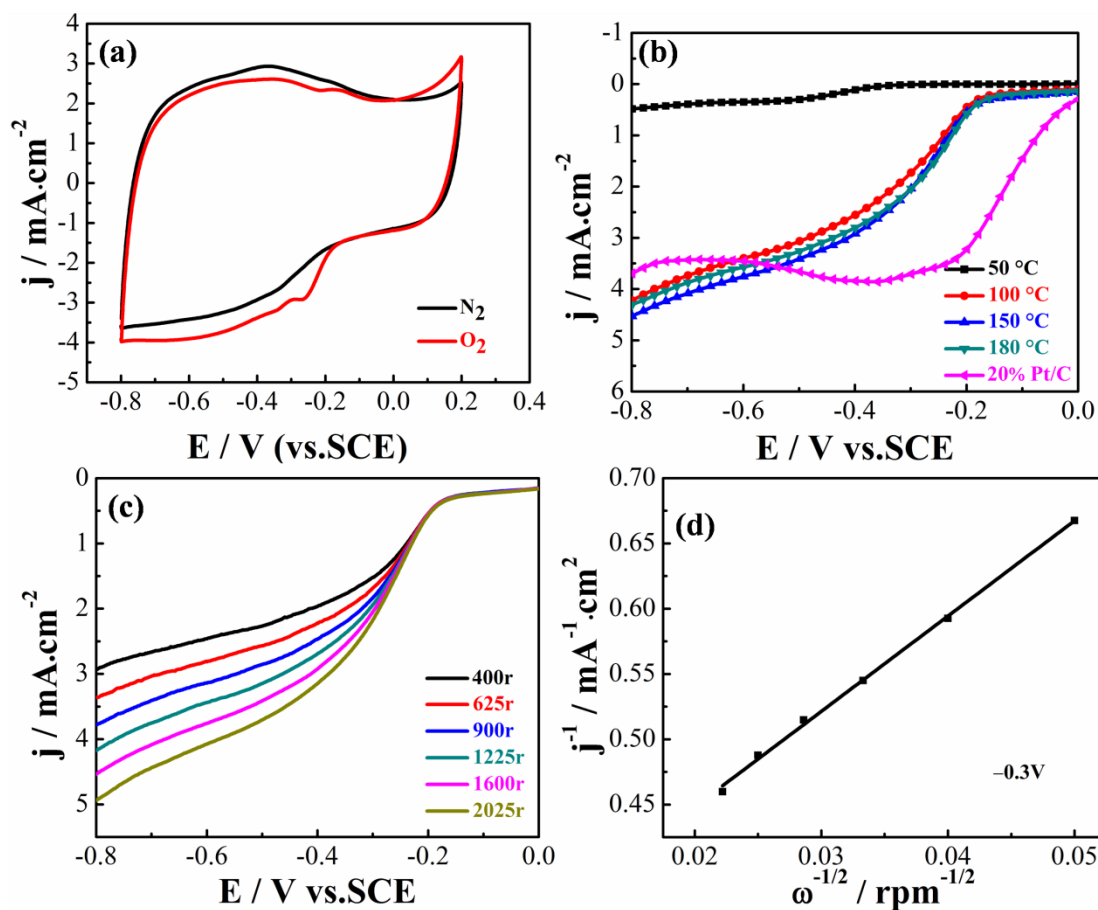


Figure 6 Cyclic voltammograms of S-N-rGO at a scan rate of 20mV s^{-1} in N_2 -saturated (black) and O_2 -saturated (red) aqueous solution of 0.1M KOH ; rotating disk electrode (RDE) voltammograms of 20% Pt/C and S-N-rGO prepared at different temperatures in an O_2 -saturated 0.1M aqueous KOH solution with a scan rate of 5 mV s^{-1} (b) at a constant rotation rate of 1600 rpm ; RDE voltammograms of S-N-rGO (c) at different rotation rates from 400 to 2025 rpm and Koutecky-Levich plot for the electrode materials at -0.3V (d).

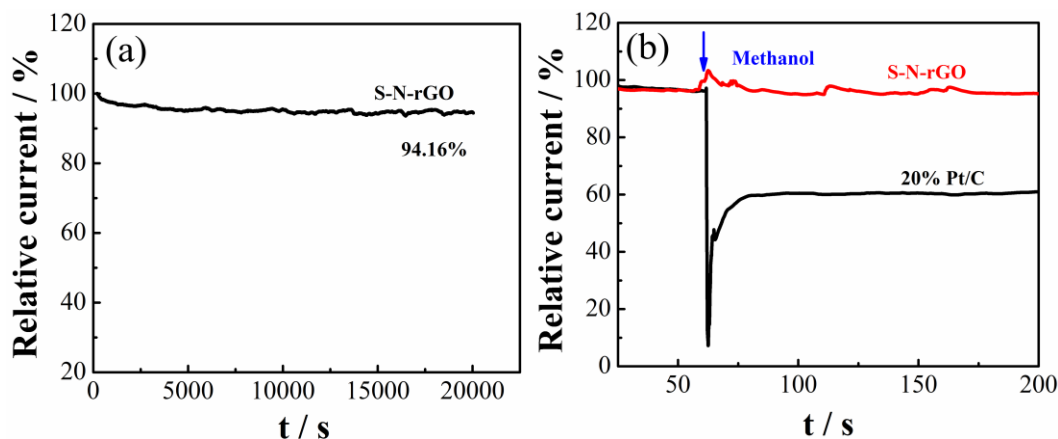


Figure 7 (a) Chronoamperometry of S-N-rGO electrode in O_2 -saturated 0.1 M KOH at -0.3V for 20000s ; (b) Chronoamperometric responses of S-N-rGO and $20\% \text{ Pt/C}$ electrodes with 3 M methanol added.

4. CONCLUSION

In summary, this work offered a green, low temperature and scalable method to prepare sulfur and nitrogen co-doped graphene by refluxing treatment of sodium sulfide, ammonium and graphene oxide. By analyzing the properties of as-obtained product, the S-N-rGO catalyst demonstrated superior catalytic activity compared to S-GO and N-GO. The excellent properties benefited from the S-N-rGO rich in pyridinic N and thiophenic S which possess perfect electronic conductivity. Even through the onset potential and half-wave potential of S-N-rGO were slightly lower than for commercial Pt/C, the stability of S-N-rGO against methanol can make it suitable for practical application. It is believed that the simple but efficient way could be further developed for the production of metal-free electrocatalyst to replace Pt/C in the area of fuel cell and metal-air battery in the future.

ACKNOWLEDGEMENTS

The authors are thankful for the support from the National Nature Science Foundation of China (Grant no. 51402150), Natural Science Foundation of Jiangsu Province (Grant no. BK20130737), the Fundamental Research Fund for the Central Universities (Grant no. NS2015061), Jiangsu Innovation Program for Graduate Education (Grant no. KYLX15-0305), the Foundation of Graduate Innovation Center in NUAA (Grant no. KFJJ20160611), the Priority Academic Program Development of Jiangsu Higher Education Institutions.

References

1. B.Y. Xia, Y. Yan, X. Wang, X.W. Lou, *Mater. Horiz.*, 1 (2014) 379.
2. S. Sharma, B.G. Pollet, *J. Power Sources*, 208 (2012) 96.
3. A. Rabis, P. Rodriguez, T.J. Schmidt, A.C.S. *Catalysis*, 2 (2012) 864.
4. J. Liu, P. Song, Z. Ning, W. Xu, *Electrocatalysis*, 6 (2015) 132.
5. M. Shao, Q. Chang, J.P. Dodelet, R. Chenitz, *Chem. Rev.*, 116 (2016) 3594.
6. Q. Shi, F. Peng, S. Liao, H. Wang, H. Yu, Z. Liu, B. Zhang, D. Su, *J. Mater. Chem. A*, 1 (2013) 14853.
7. A.M. Gomez-Marin, R. Rizo, J.M. Feliu, *Catalysis Science & Technology*, 4 (2014) 1685.
8. J. Wu, H. Yang, *Acc. Chem. Res.*, 46 (2013) 1848.
9. X.Q. Huang, Z.P. Zhao, L. Cao, Y. Chen, E.B. Zhu, Z.Y. Lin, M.F. Li, A.M. Yan, A. Zettl, Y.M. Wang, X.F. Duan, T. Mueller, Y. Huang, *Science*, 348 (2015) 1230.
10. X. Tian, J. Luo, H. Nan, H. Zou, R. Chen, T. Shu, X. Li, Y. Li, H. Song, S. Liao, R.R. Adzic, *J. Am. Chem. Soc.*, 138 (2016) 1575.
11. S. Zhang, Y. Shao, G. Yin, Y. Lin, *Applied Catalysis B: Environmental*, 102 (2011) 372.
12. G. Wu, N.H. Mack, W. Gao, S. Ma, R. Zhong, J. Han, J.K. Baldwin, P. Zelenay, *A.C.S. Nano*, 6 (2012) 9764.
13. L.T. Qu, Y. Liu, J.B. Baek, L.M. Dai, *A.C.S. Nano*, 4 (2010) 1321.
14. K. Qu, Y. Zheng, S. Dai, S.Z. Qiao, *Nanoscale*, 7 (2015) 12598.
15. H.J. Cui, H.M. Yu, J.F. Zheng, Z.J. Wang, Y.Y. Zhu, S.P. Jia, J. Jia, Z.P. Zhu, *Nanoscale*, 8 (2016) 2795.
16. M. Zhang, L. Dai, *Nano Energy*, 1 (2012) 514.
17. Z. Yang, Z. Yao, G.F. Li, G.Y. Fang, H.G. Nie, Z. Liu, X.M. Zhou, X. Chen, S.M. Huang, *A.C.S. Nano*, 6 (2012) 205.

18. S. Wang, L. Zhang, Z. Xia, A. Roy, D.W. Chang, J.B. Baek, L. Dai, *Angew. Chem. Int. Ed. Engl.*, 51 (2012) 4209.
19. J. Tai, J. Hu, Z. Chen, H. Lu, *R.S.C. Adv.*, 4 (2014) 61437.
20. S. Bag, B. Mondal, A.K. Das, C.R. Raj, *Electrochim. Acta*, 163 (2015) 16.
21. S. Dou, A. Shen, Z. Ma, J. Wu, L. Tao, S. Wang, *J. Electroanal. Chem.*, 753 (2015) 21.
22. J. Jin, F. Pan, L. Jiang, X. Fu, A. Liang, Z. Wei, J. Zhang, G. Sun, *A.C.S. Nano*, 8 (2014) 3313.
23. Z. Zhao, Z. Xia, *M.R.S. Advances*, 1 (2016) 421.
24. Z. Wang, P. Zuo, L. Fan, J. Han, Y. Xiong, G. Yin, *J. Power Sources*, 311 (2016) 68.
25. Y. Wang, X. Zhang, A. Li, M. Li, *Chem. Commun. (Camb)*, 51 (2015) 14801.
26. H. Zhang, X. Liu, G. He, X. Zhang, S. Bao, W. Hu, *J. Power Sources*, 279 (2015) 252.
27. S.N. Bhange, S.M. Unni, S. Kurungot, *J. Mater. Chem. A*, 4 (2016) 6014.
28. J. Wu, X. Zheng, C. Jin, J. Tian, R. Yang, *Carbon*, 92 (2015) 327.
29. Z. Liu, X. Fu, M. Li, F. Wang, Q. Wang, G. Kang, F. Peng, *J. Mater. Chem. A*, 3 (2015) 3289.
30. J. Xu, Y. Zhao, C. Shen, L. Guan, *A.C.S. Appl. Mater. Interfaces*, 5 (2013) 12594.
31. Z.H. Sheng, H.L. Gao, W.J. Bao, F.B. Wang, X.H. Xia, *J. Mater. Chem.*, 22 (2012) 390-395.
32. F. Pan, J. Jin, X. Fu, Q. Liu, J. Zhang, *A.C.S. Appl. Mater. Interfaces*, 5 (2013) 11108.
33. M. Wu, Z. Dou, J. Chang, L. Cui, *R.S.C. Adv.*, 6 (2016) 22781.
34. W.N. Yan, X.C. Cao, J.H. Tian, C. Jin, K. Ke, R.Z. Yang, *Carbon*, 99 (2016) 195.
35. Y. Su, Y. Zhang, X. Zhuang, S. Li, D. Wu, F. Zhang, X. Feng, *Carbon*, 62 (2013) 296.
36. S.M. Jung, E.K. Lee, M. Choi, D. Shin, I.Y. Jeon, J.M. Seo, H.Y. Jeong, N. Park, J.H. Oh, J.B. Baek, *Angew. Chem. Int. Ed. Engl.*, 53 (2014) 2398.
37. D.C. Marcano, D.V. Kosynkin, J.M. Berlin, A. Sinitskii, Z. Sun, A. Slesarev, L.B. Alemany, W. Lu, J.M. Tour, *A.C.S. Nano*, 4 (2010) 4806.
38. S. Chao, Q. Cui, Z. Bai, K. Wang, L. Yang, *Electrochim. Acta*, 177 (2015) 79.
39. D.H. Guo, R. Shibuya, C. Akiba, S. Saji, T. Kondo, J. Nakamura, *Science*, 351 (2016) 361.
40. C. Domínguez, F.J. Pérez-Alonso, S.A. Al-Thabaiti, S.N. Basahel, A.Y. Obaid, A.O. Alyoubi, J.L. Gómez de la Fuente, S. Rojas, *Electrochim. Acta*, 157 (2015) 158.
41. S. Gao, H. Liu, K. Geng, X. Wei, *Nano Energy*, 12 (2015) 785.
42. F. Buckel, F. Effenberger, C. Yan, A. Goltzhauser, M. Grunze, *Adv. Mater.*, 12 (2000) 901.
43. X. Li, H. Wang, J.T. Robinson, H. Sanchez, G. Diankov, H. Dai, *J. Am. Chem. Soc.*, 131 (2009) 15939.
44. Y. Zhu, S. Murali, W. Cai, X. Li, J.W. Suk, J.R. Potts, R.S. Ruoff, *Adv. Mater.*, 22 (2010) 3906.
45. X. Wang, J. Wang, D. Wang, S. Dou, Z. Ma, J. Wu, L. Tao, A. Shen, C. Ouyang, Q. Liu, S. Wang, *Chem Commun (Camb)*, 50 (2014) 4839
46. S.A. Wohlgemuth, R.J. White, M.G. Willinger, M.M. Titirici, M. Antonietti, *Green Chemistry*, 14 (2012) 1515.
47. A.K. Samantara, S. Chandra Sahu, A. Ghosh, B.K. Jena, *J. Mater. Chem. A*, 3 (2015) 16961.
48. X. K. Kong, C. L. Chen, Q. W. Chen, *Chem Soc Rev.*, 43 (2014) 2841.
49. Z. Liu, H. Nie, Z. Yang, J. Zhang, Z. Jin, Y. Lu, Z. Xiao, S. Huang, *Nanoscale*, 5 (2013) 3283.